

CONCENTRIC CRATER FILL: RATES OF GLACIAL ACCUMULATION, INFILLING AND DEGLACIATION IN THE AMAZONIAN AND NOACHIAN OF MARS. James L. Fastook¹ and James W. Head², ¹University of Maine, Orono, ME 04469, fastook@maine.edu, ²Brown University, Providence, RI 02912.

Introduction: Concentric Crater Fill (CCF) [1-6] is one of many features on Mars that are thought to either contain ice, or to have been formed by a glaciological process that involved the deformation and movement of a significant thickness of ice, emplaced during a climatic period when the obliquity and other spin-orbital parameters favored deposition in areas where ice is not currently stable [7-10]. Such features include Tropical Mountain Glaciers [11-15], Lobate Debris Aprons, and Lineated Valley Fill [12, 16-28]. Others, such as Pedestal, Perched, and Excess Ejecta Craters [29-32], record the presence of widespread mantling. Features that preserve ice presumably do so by covering the ice surface with a thin (< 15 m) layer of debris [33-37]. In all cases, understanding the mechanism that leads to the formation of these features provides insights into the state of the current climate and how it must have changed in the past.

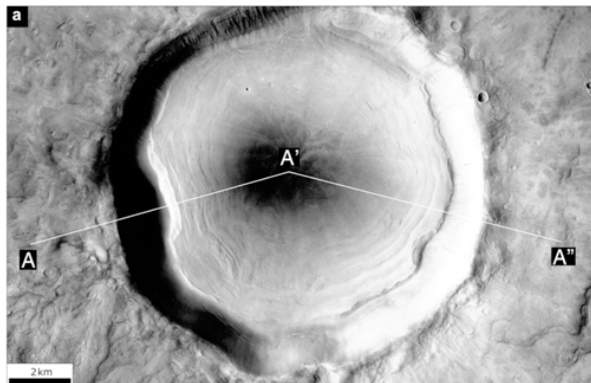


Figure 1: P14_006570_2241 HRSC CCF Crater used as a target.

Although there are many hypotheses of how CCF might have formed (see [1,3] for a comprehensive discussion), in this we assume that CCF is composed largely of debris-covered ice that at some point flowed and then sublimated, producing the observed flow-like debris cover (Fig. 1, [3]), and that the age is Amazonian [2,3,5,6]. Pedestal Craters record a repeating, transient, widespread ice mantling, and even provide estimates of the thickness of this layer [30-32]. The question then is how does a thin mantling layer flow in such a way as to fill CCF craters with ice to a depth of more than a km? Could it have happened during a single, presumably most recent, episode of mantling,? Or, is it a cumulative gathering of material into the crater during frequent repeated episodes of mantling?

Results: We use a 1D flowband model based on the University of Maine Ice Sheet Model [38-40], coupled with an advection-based model of surface debris transport. We assume that whenever the ice surface drops be-

low the crater rim crest, debris is deposited locally on the ice surface in the crater interior, and then transported with the movement of the downward and inward-flowing ice. To characterize the two cases we perform experiments to see how long it takes for a modeled crater to fill to a level that matches the Fig. 1 observed CCF crater [3]. Fig. 2 shows the two cases.

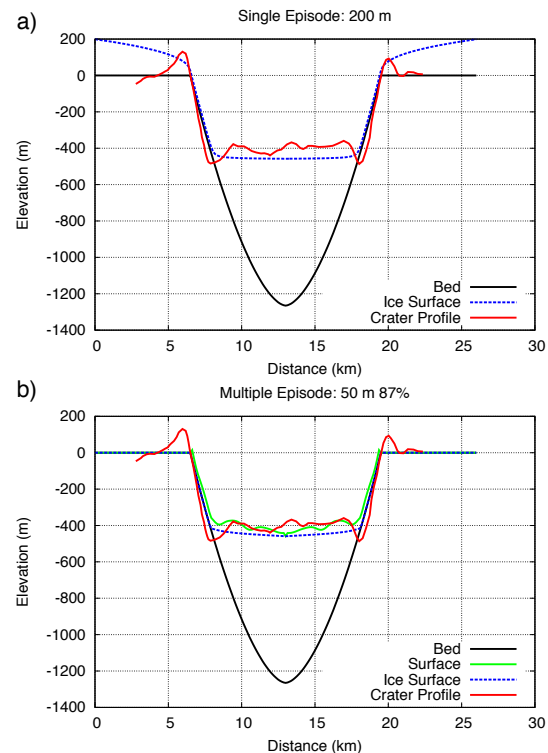


Figure 2: a) A single episode of mantling 200 m thick that flows into the crater. b) Multiple episodes of mantling 50 m thick driven by an obliquity scenario.

Single Persistent Episode: For the single-episode case, we begin with a mantling layer 200 m thick. We hold the thickness to be fixed at the boundary of our model domain. As ice is removed from the top of the crater wall as it flows into the crater, the lowered surface provides a sloping surface from the fixed domain edge that can draw ice from outside the model domain. A comparison between the model results (black) and the observed CCF crater profile (red) is shown in Fig. 2a. At a temperature of 215 K this process takes ~ 1.1 Gyr for the model crater to fill to the level in the CCF crater. **Given the time required for the crater to fill to an appropriate level, we interpret this candidate scenario as being unrealistic for CCF formation.**

Multiple Transient Episodes: For the multiple-episode case shown in Fig. 2b, the model is driven with

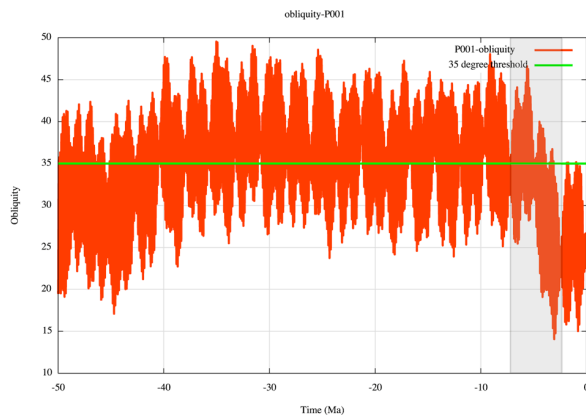


Figure 3: Obliquity scenario used to drive multiple episode case.

the obliquity scenario shown in Fig. 3 [10] with repeated cycles of ice-layer formation. In this scenario the mean obliquity is relatively high from 40 Myr until 5 Myr, at which point it drops to its current value. We chose an obliquity threshold of 35° (the green line in Fig. 3), above which we consider the ice layer to have a positive mass balance of 1 mm/yr, typical of GCM results for high obliquity [8, 9], and below which we ablate the ice, with the rate depending on the amount of debris armoring the surface [41]. Prior to 5 Myr, the mean obliquity is above this threshold, although there are regular excursions to lower obliquity during which the unarmored portion of the layer would partially or completely sublimate away. After 5 Myr, the mean obliquity drops below the 35° threshold, although there continue to be briefer and less frequent excursions above the threshold, during which an ice layer is deposited. Note that after 3 Myr there are no further obliquity excursions that exceed the threshold, and that the ice layer is in a continual state of sublimation.

We limit the deposited layer (Fig. 4a) to a specified thickness of 50 m by turning off the accumulation when the layer volume has reached its “supply-limited” value. In the case of episodic layer formation, the source of the ice that flows into the crater will be that deposited on the steep crater walls as the layer is draped over the terrain during each of many episodes (Fig. 4b). Even at a temperature of 215 K, ice is able to flow down the steep slopes of the crater walls into the crater interior, resulting in thicker ice there and thinner ice on the slopes and inter-crater terrain. During low obliquity periods of negative mass balance (Fig. 4c), ice on the steeper unarmored slopes (and rim and inter-crater terrain) may be entirely removed, but the thicker ice in the crater interior, now below the height of the crater walls and covered by armoring debris, may not all be removed and the crater can fill with ice and transported debris (Fig. 4e,f). Indeed, as much as 3% of the crater volume can be deposited in each obliquity episode that exceeds the threshold, rapidly filling the crater to its rim. What is deposited in the crater must, however, survive the period of

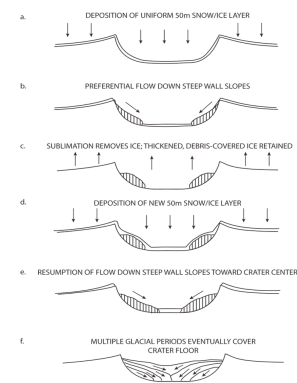


Figure 4: Schematic of multiple-episode CCF formation

continuous sublimation that occurs after 3 Myr when there are no obliquity episodes that exceed the threshold (Fig. 3). The start-and-stop nature of the forward motion of the ice dictates that the transported debris layer will not be uniform in thickness and this is apparent in the modeled green line surface of Fig. 2b. **The final state of this 50 Myr simulation driven by an obliquity signal results in ~800 m of fill in less than one-twentieth the time it takes for an infinite persistent layer to flow into the crater to a comparable depth.**

Application to the Noachian: Wordsworth et al. [42] recently proposed that the Late Noachian climate resulted in an “icy highlands” environment in which snow and ice blanketed much of the southern uplands of Mars [42]. **This same mechanism that operated in the Amazonian would also operate on craters in the Late Noachian icy highlands [43]; these craters would, be subjected to similar repetitive mantling events that would carry debris into the craters, shallowing them and degrading the crater rim crests [44].**

References: 1. M. Kreslavsky, J. Head (2006) *Meteorit. Planet. Sci.*, 41:1633; 2. J. Levy et al. (2009) *Icarus*, 202(2):462; 3. J. Levy et al. (2010) *Icarus*, 209(2):390; 4. J. Dickson et al. (2012) *Icarus*, 219(2):723; 5. M. Beach, J. Head (2012) *LPS43 #1140*; 6. M. Beach, J. Head (2013) *LPS44 #1161*; 7. R. Haberle et al. (2003) *Icarus*, 161(1):66; 8. F. Forget et al. (2006) *Science*, 311(5759):368; 9. J.-B. Madeleine et al. (2009) *Icarus*, 203(2):390; 10. J. Laskar et al. (2004) *Icarus*, 170(2):343; 11. J. Head, D. Marchant (2003) *Geology*, 31(7):641; 12. J. Head et al. (2005) *Nature*, 434:346; 13. D. Shean et al. (2005) *JGR*, 110:E05001; 14. D. Shean et al. (2007) *JGR*, 112:E03004; 15. S. Kadish et al. (2008) *Icarus*, 197:84; 16. B. Lucchitta (1984) *JGR*, 89(s02):B409; 17. N. Mangold (2003) *JGR*, 108(E4):8021; 18. T. Pierce, D. Crown (2003) *Icarus*, 163(1):46; 19. H. Li et al. (2005) *Icarus*, 176(2):382; 20. J. Head et al. (2006a) *Earth Planet. Sci. Lett.*, 241(3-4):663; 21. J. Head et al. (2006b) *GRL*, 33(8):L08S03; 22. J. Head et al. (2010) *Earth Planet. Sci. Lett.*, 294(3-4):306; 23. J. Levy et al. (2007) *JGR*, 112:E08004; 24. L. Ostrach et al. (2008) *LPS39, #2422*; 25. G. Morgan et al. (2009) *Icarus*, 202(1):22; 26. D. Baker et al. (2010) *Icarus*, 207(1):186; 27. J. Dickson et al. (2008) *Geology*, 36(5):411; 28. J. Dickson et al. (2010) *Earth Planet. Sci. Lett.*, 294(3-4):332; 29. S. Kadish, J. Head (2011) *Icarus*, 215(1):34; 30. S. Kadish, J. Head (2011) *Icarus*, 213(2):443; 31. S. Kadish et al. (2009) *JGR*, 114:E10001; 32. S. Kadish et al. (2010) *Icarus*, 210(1):92; 33. J. Holt et al. (2008) *Science*, 21:1235; 34. J. Plaut et al. (2009) *GRL*, 36(2):L02203; 35. D. Marchant et al. (2002) *GSA Bulletin*, 114(6):718; 36. D. Marchant et al. (2007) *10th Int. Symp. on Ant. Earth Sci.*, USGS OFR-2007:1; 37. D. Kowalewski et al. (2011) *Geomorphology*, 126(1-2):159; 38. J. Fastook (1993) *Comput. Sci. and Eng.*, 1(1):55; 39. J. Fastook et al. (2004) *LPS35, #1352*; 40. J. Fastook et al. (2008) *Icarus*, 198:305; 41. J. Fastook et al. (2013) *Icarus*, 228:54; 42. R. Wordsworth et al. (2013) *Icarus*, 222:1; 43. J. Fastook and J. Head (2014) *LPS45, #1115*; 44. D. Weiss, J. Head (2014) *LPS45, #1077*.